AIP Advances

Interfacial coupling-induced distinct magnetic structure in $La_{1/2}Sr_{1/2}CoO_{2.5+\delta}$/ $La_{2/3}Sr_{1/3}MnO_3$/ $La_{1/2}Sr_{1/2}CoO_{2.5+\delta}$ heterostructure

Cite as: AIP Advances **9**, 035130 (2019); https://doi.org/10.1063/1.5079958
Submitted: 05 November 2018 . Accepted: 21 January 2019 . Published Online: 15 March 2019

Jine Zhang, Wei Wang, Jing Zhang, Xiaobing Chen, Furong Han, Hailin Huang, Hui Zhang, Baogen Shen, Richeng Yu, and Jirong Sun

Interfacial coupling-induced distinct magnetic structure in $La_{1/2}Sr_{1/2}CoO_{2.5+\delta}/La_{2/3}Sr_{1/3}MnO_3/La_{1/2}Sr_{1/2}CoO_{2.5+\delta}$ heterostructure

Cite as: AIP Advances 9, 035130 (2019); doi: 10.1063/1.5079958
Presented: 15 January 2019 • Submitted: 5 November 2018 •
Accepted: 21 January 2019 • Published Online: 15 March 2019

Jine Zhang,[1,2] Wei Wang,[1,2] Jing Zhang,[1,2] Xiaobing Chen,[1,2] Furong Han,[1,2] Hailin Huang,[1,2] Hui Zhang,[1,2] Baogen Shen,[1,2] Richeng Yu,[1,2] and Jirong Sun[1,2,a)]

AFFILIATIONS

[1]Beijing National Laboratory for Condensed Matter Physics & Institute of Physics, Chinese Academy of Sciences, Beijing 100190, People's Republic of China

[2]School of Physical Sciences, University of Chinese Academy of Sciences, Beijing 100049, People's Republic of China

Note: This paper was presented at the 2019 Joint MMM-Intermag Conference.
[a)]**Correspondence author:** jrsun@iphy.ac.cn

ABSTRACT

The interfacial coupling between electron correlated complex oxides opens a promising avenue for achieving new forms of magnetism that arises as a consequence of charge transfer, orbital reconstruction and symmetry-breaking. Herein we reported a distinct magnetic structure in $La_{2/3}Sr_{1/3}MnO_3$ (LSMO) film sandwiched between $La_{1/2}Sr_{1/2}CoO_{2.5+\delta}$ (LSCO) bilayer grown on (001)-oriented $SrTiO_3$ substrates. It is found that the LSMO layer of heterostructure contains two independent components that are respectively free layer (free-LSMO) and coupled layer with LSCO (coupled-LSMO). The easy axis of the free-LSMO is in-plane, while it is out-of-plane directed for the coupled-LSMO layer. The thickness of these two parts in the LSMO layer are 4uc and 12uc respectively. This is in sharp contrast to the single LSMO layer on STO, for which the easy axis is always in film plane. Different from LSMO, the easy axis of LSCO is in-plane and is ferromagnetically coupled with LSMO. This distinct magnetic structure could be ascribed to orbital reconstruction due to symmetry-mismatch at interfaces.

I. INTRODUCTION

ABO_3-typed transition metal oxides exhibit a wide range of exotic physical properties that arise as a consequence of strong correlations between electron, spin, orbital and lattice. As a typical ferromagnetic metal oxide, $La_{2/3}Sr_{1/3}MnO_3$ (LSMO) is attractive for its high Curie temperature,[1] colossal magnetoresistance effect[2] and tunable spin orientation.[3–6] Generally, the spin of a single LSMO film can be tuned by lattice strain. For example, the easy axis of LSMO is in-plane when it is tensely strained,[3,4] while it aligns along the out-of-plane direction when the film is compressively strained.[3,4] However, emergent phenomenon appears when LSMO is grouped with other perovskite oxides together via interface engineering.[6–10] As reported by Hoffman et al.,[6] the magnetic structure is noncollinear in the LSMO/$LaNiO_3$ superlattices. As shown by Liao et al.,[7] a reorientation of the easy axis in film plane by an angle of 90° occurs for LSMO after inserting a $SrTiO_3$ layer between LSMO and $NdGaO_3$ substrate.

While most of previous works focused on the perovskite/perovskite type heterostructures. Recently, Zhang *et al.*[10] revealed the new perovskite/brownmillerite (LSMO/$LaCoO_{2.5}$) heterointerfaces and the symmetry-mismatch induced by it results in the perpendicular magnetic anisotropy (PMA) of LSMO even it is in a tensile state. Herein, we are interested in LSMO/$La_{0.5}Sr_{0.5}CoO_{2.5+\delta}$ (LSCO) heterostructure since LSCO is more likely to form brownmillerite.[11,12] We also observed the PMA and further studied the distinct magnetic structure of LSCO/LSMO/LSCO. It's found that the LSMO layer contains two independent parts that are not coupled with (free-LSMO) and coupled with LSCO (coupled-LSMO), the spins of the free-LSMO prefer to align laterally, while the ones of

the coupled-LSMO orientate perpendicularly. The thickness of these two parts in LSMO layer are 4uc and 12uc respectively. This is different from the single LSMO layer on STO, which exhibits an in-plane easy axis.

II. EXPERIMENTS

LSCO(20uc)/LSMO(16uc)/LSCO(20uc) heterostructure was fabricated on TiO_2-terminated (001)-STO single crystal substrate ($3\times5\times0.5mm^3$) by pulsed laser deposition (KrF Excimer laser, wavelength = 248 nm). The growth temperature was maintained at 700 °C and the oxygen pressure was 40 Pa. Surface morphology of heterostructure was measured by atomic force microscope (AFM, SPI 3800N, Seiko). Crystal structure was determined by the Bruker X-ray diffractometer equipped with thin film accessories (D8 Discover, Cu Kα radiation). Magnetic measurements were performed on Quantum Designed Vibrating Sample Magnetometer.

III. RESULTS AND DISCUSSION

The LSCO(20uc)/LSMO(16uc)/LSCO(20uc) heterostructure is of high quality. Figure 1(a) presents the surface morphology of the heterostructure. The film is rather flat with a root mean squared roughness of ~0.7 nm. Figure 1(b) demonstrates the x-ray diffraction spectrum which is different from that of either a single LSCO (3.83 Å, marked by a red arrow) or a single LSMO (3.87 Å, marked by a black arrow). It is somewhat complex, composed of a series of coherent diffraction/interference peaks that are combined result of the three layers. The clear reflections indicate a high crystal quality of the films.

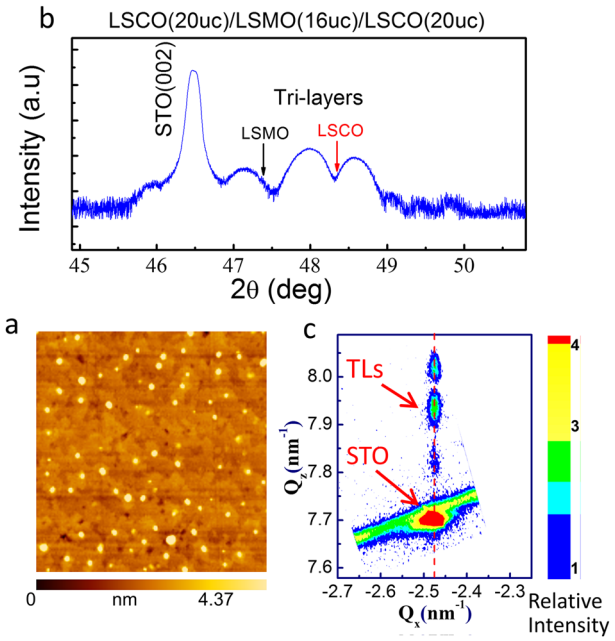

FIG. 1. (a) Surface morphology of the trilayers. (b) X-ray diffraction pattern for the film. Red (Black) arrow denotes the expected peak position of single LSCO (LSMO). (c) Reciprocal space mapping of the (-103) reflection of the trilayers ("TLS").

To reveal lattice strains, we measured the reciprocal space mapping of the (-103) reflection (Figure 1(c)). The most notable characteristic is the vertical alignment of the reflections from the film and the substrate. In addition to implying a coherent epitaxial growth, this result indicates that the film shares exactly the same in-plane lattice constant with substrate (a=3.905Å) which is apparently larger than the bulk one (3.83Å for LSCO; 3.87Å for LSMO), i.e., the heterostructure is tensely strained.

To investigate the magnetic structure of the heterostructure, the thermomagnetic curves were measured in Figure 2(a). Intriguingly, the LSMO layer when coupled with LSCO displays an abnormal perpendicular magnetic anisotropy (PMA) at low temperatures, though easy axis of the single LSMO layer lies in film plane.[3,4] Different from LSMO, as shown the enlarged thermomagnetic curves at the fixed field of 0.01T in Figure 2(b), the easy axis of LSCO is in film plane. The magnetic signal of LSCO was observed below 140K (T_C of LSCO), applied in-plane (IP) fields. In contrast, the magnetic signal of LSCO can hardly be seen along out-of-plane (OP) direction. This magnetic orientation of the LSCO layer in heterostructure is similar to that of the single layer. Simply extrapolating the high temperature part of the IP M–T curve (>140 K) down to 10 K (the red dash line), the magnetization of the LSMO layer can be estimated. Purple areas highlight the difference of the magnetic moment of LSMO layer along two measuring directions: the OP magnetic moments are significantly higher than IP ones, indicating that the total magnetic moments of LSMO prefer to align perpendicularly. Here, The T_C (140k) of $La_{1/2}Sr_{1/2}CoO_{2.5+\delta}$ is lower than that (200K) of $La_{1/2}Sr_{1/2}CoO_3$,[13] since the ferromagnetic order is reduced for the oxygen deficiency.

To quantify the magnetic anisotropy, we extracted the M-H curves at the fixed temperature of 10 K from the data in Figure 2(a). Shown in Figure 2(c) is M-H curves along IP or OP directions. The output of the calculation of the purple area is the anisotropy constant $K_A=1.3\times10^5$ erg/cm^3. Positive value denotes the PMA. This PMA is further evidenced by a direct measurement of magnetic loops with IP or OP fields (Figure 2(d)). Here, the measurements were conducted at 140 K to avoid magnetic contribution of the LSCO layers.

Interestingly, the magnetic moments of the LSMO layer prefer to align along OP direction even the sample is tensely strained. To get further information on magnetic structure, we carefully analyzed the magnetic loops. Figure 3a demonstrates the M-H relationship of heterostructure along two directions measured at 10 K: the OP magnetic loop exhibits a simple easy axis behavior, whereas the IP loop is much more complex, showing a thin middle waist. The M-H relations were further decomposed into two different magnetic loops, with different coercivity forces. In general, the magnetic loop with a large coercivity force comes from LSCO while the one with small coercivity force stems from LSMO (Figure 3b). We measured the magnetic loop of single LSCO(40uc) with IP magnetic fields, obtaining a coercivity force 1.8T that is consistent with the decomposition result 1.8T. We also measured the LSMO (16uc) single film (Figure 3c), and found a difference between measured and deduced magnetic loops for the LSMO layer. It is obvious that the LSMO in heterostructure behaves differently from its single layer counterpart. A further analysis shows that the M-H relation of LSMO layer in heterostructure can be decomposed into two independent loops that we ascribed to free LSMO layer (free-LSMO) and coupled LSMO layer (coupled-LSMO), respectively. Figure 3d and 3e

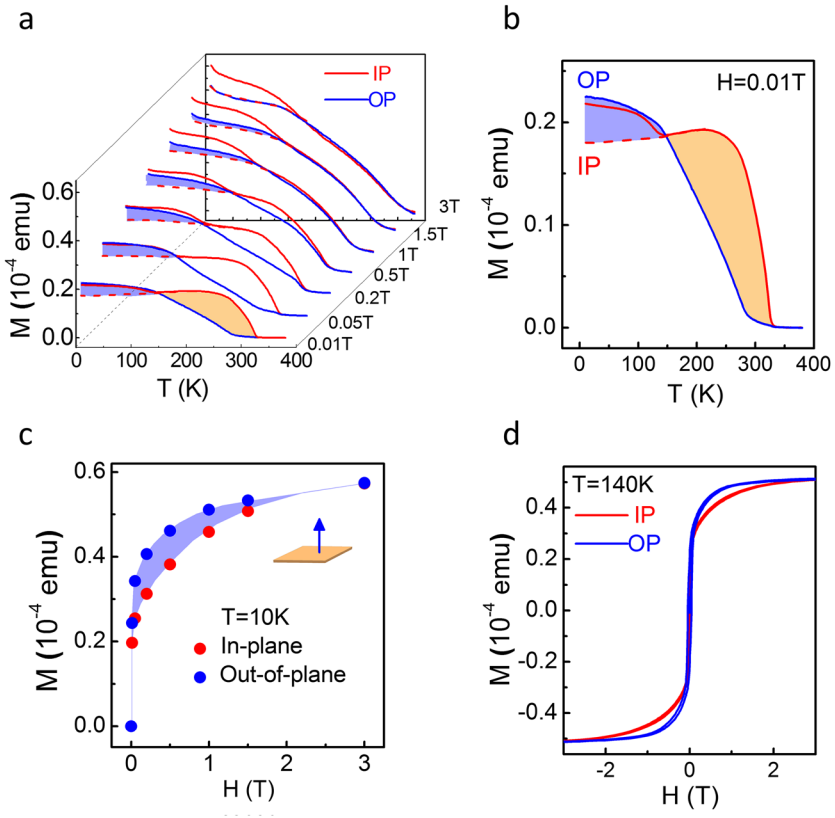

FIG. 2. (a) Temperature dependence of the magnetization after field-cooling (FC) for LSCO(20uc)/LSMO(16uc)/LSCO(20uc) heterostructure, applied in-plane (IP) or out-of-plane (OP) fields. Here, all the in-plane direction is symmetry equivalent. (b) The enlarged thermomagnetic curves of heterostructure at H=0.01T. (c) Magnetic moment as a function of applied fields, extracted from the data in (a) at T=10 K. Shaded area corresponds to the energy required to orientate magnetic moment towards the IP direction. (d) A direct measurement of magnetic loops with IP and OP fields, conducted at 140 K.

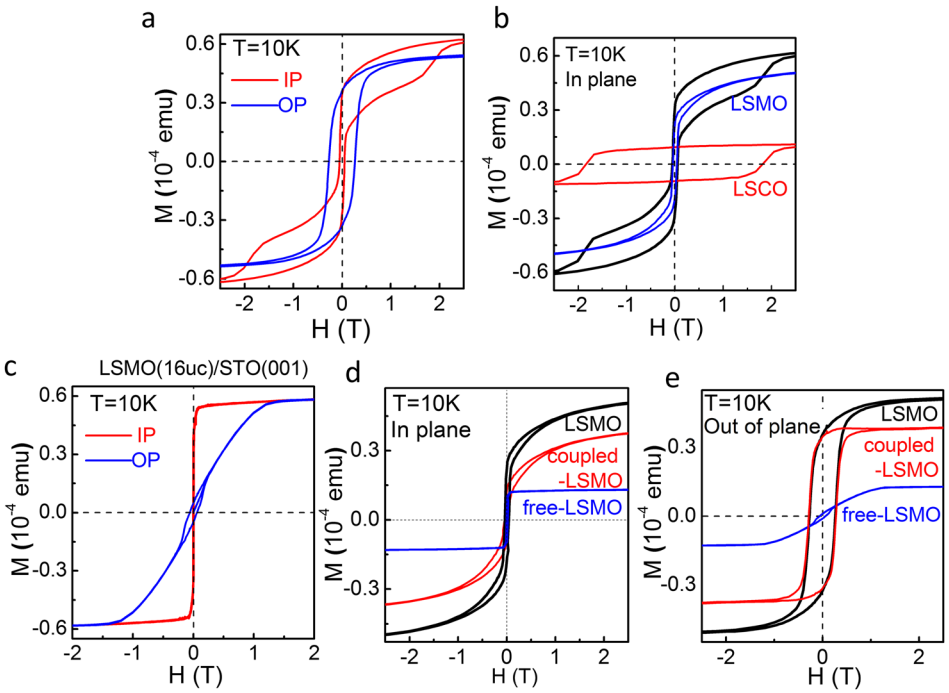

FIG. 3. (a) Magnetic loops of the LSCO/LSMO/LSCO, measured at 10 K using IP or OP fields. (b) Decomposition of the IP magnetic loop in (a) into two loops associated with LSMO and LSCO respectively. (c) Magnetic loops of LSMO(16uc)/STO(001). (d)-(e) A further decomposition of the magnetization of LSMO (black curve) into two independent loops associated with free-LSMO and coupled-LSMO, respectively, here (d) or (e) correspond to IP or OP magnetic loop.

present the corresponding results with in-plane or out-of-plane fields.

Obviously, the free component of LSMO layer in LSCO/LSMO/LSCO was not affected by LSCO, with its easy axis aligning laterally as usual. However, the coupled-LSMO component has been modified by neighboring LSCO, and its spin orientation is perpendicular. From respective contributions to magnetic moments, a direct calculation yields that the thickness of the free to coupled layers is 4uc and 12uc respectively. It means that the two LSCO(20uc) layers can affect the spin reorientation of LSMO with the thickness of up to 12uc.

Figure 4(a) presents the main and minor magnetic loops to study the coupling between LSCO and LSMO. The enlarged minor loop is shown in Figure 4(b). The Red (blue) minor loop is recorded by saturating the sample and then a cycling magnetic field along +0.5T(-0.5T)→-0.5T(+0.5T)→+0.5T(-0.5T). Here, we choose the field of 0.5T to confirm that the magnetic moments of LSMO change with magnetic field and LSCO keeps the magnetic orientation. If there is no interaction between LSMO and LSCO, the center of the minor loop should be in zero field. As marked by the red (blue) cross, the center of the minor loop deviates from the origin by a field of ~0.024 T. indicating a negative exchange bias. This is that the interlayer coupling between LSCO and LSMO is Ferromagnetic (FM) in nature.

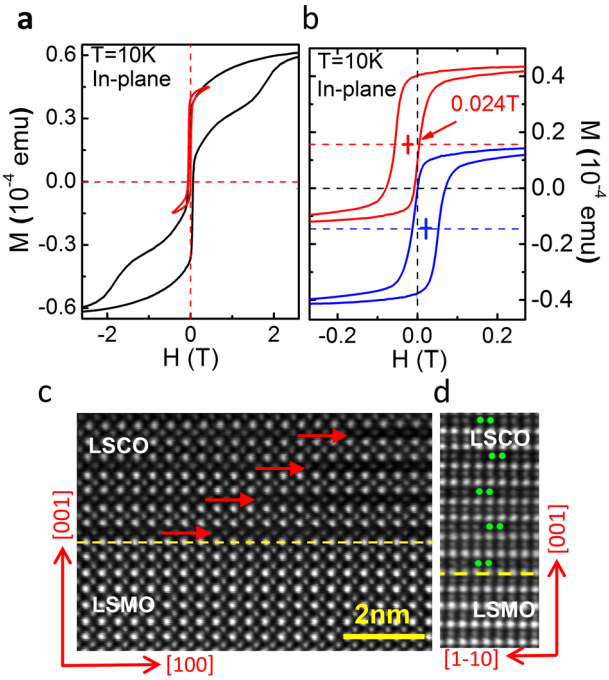

FIG. 4. (a) A comparison of the main magnetic loop and the minor loop (b) The enlarged minor loop (red loop). The Red (blue) minor loop is recorded by saturating the sample under a field of +3T(-3T) and then a cycling magnetic field along the path of +0.5T(-0.5T)→-0.5T(+0.5T)→+0.5T(-0.5T). (c)-(d) HAADF images of the LSCO/LSMO/LSCO, recorded along [001] and [110] zone respectively. The interface between LSCO and LSMO is marked by yellow dashed lines. Red arrows denote dark stripes. Breath mode lattice distortion can be clearly seen (marked by green dots).

A further issue to be addressed is that how LSCO affects LSMO. To elucidate the mechanism, the lattice structure of the multilayer is further studied. Figure 4(c) and 4(d) shows the High-angle annular dark-field (HAADF) image of LSCO/LSMO/LSCO, recorded along [001] and [110] zone respectively. The brighter and fainter dots correspond to the La/Sr and Mn/Co atomic rows, respectively. Here, the most remarkable findings are the parallel dark stripes appear every other column in the LSCO layers and the breath mode lattice distortion (marked by green dots) for the Co ions in dark stripes. These are the fingerprint of brownmillerite phase.[11,14] Therefore, the interface of perovskite/brownmillerite is fabricated and the interfacial MnO_6 octahedra is connected to CoO_4 tetrahedra (Figure 4c), As reported by Zhang et al.,[10] which will result in that the oxygen atoms connecting octahedral and tetrahedron move to the direction of CoO_4 tetrahedra, causing the longitudinal elongation of MnO_6 octahedra. This effect will cause a preferred occupation of the $d_{3z2\text{-}r2}$ orbital.[10] In this case, the orbital momentum could be finite in the normal direction of the film plane.[15] According to the Bruno model,[16,17] the easy axis prefers to take the direction of the orbital momentum. That's why the PMA.

As demonstrated above, the interface of perovskite/brownmillerite induced the PMA. That means the PMA should be enhanced by the formation of more brownmillerite phase. The content of δ in $La_{0.5}Sr_{0.5}CoO_{2.5+\delta}$ implying the density of brownmillerite structure. Therefore, we can control the PMA by tuning δ.

IV. CONCLUSIONS

In summary, high quality LSCO/LSMO/LSCO has been fabricated on STO(001) substrate. Interfacial coupling-induced distinct magnetic structure was resulted in LSMO sandwiched by LSCO layers, decomposed into a free layer and a coupled layer. The free layer of LSMO prefers to align in film plane while the coupled-layer orientates perpendicularly. According to their respective magnetic contributions, a direct calculation yields the thickness of the free to coupled layers is 4uc and 12uc respectively. In contrast, magnetic moments of the LSCO layer remain in-plane orientated. The magnetic coupling between LSCO and LSMO is FM in nature. The present work shows the great potential of interface engineering to explore the distinct spin texture for the complex oxides.

ACKNOWLEDGMENTS

This work has been supported by the National Basic Research of China (2016YFA0300701, 2017YFA0206300 and 2014CB920902), the National Natural Science Foundation of China (11520101002, 51590880, and 11674378), and the Key Program of the Chinese Academy of Sciences.

REFERENCES

[1] I. Bergenti, V. Dediu, M. Cavallini, E. Arisi, A. Riminucci, and C. Taliani, Current Applied Physics **7**, 47 (2007).
[2] Y. Tokura, Reports on Progress in Physics **69**, 797 (2006).
[3] F. Tsui, M. C. Smoak, T. K. Nath, and C. B. Eom, Applied Physics Letters **76**, 2421 (2000).

[4]A. M. Haghiri-Gosnet, J. Wolfman, B. Mercey, Ch. Simon, P. Lecoeur, M. Korzenski, M. Hervieu, R. Desfeux, and G. Baldinozzi, Journal of Applied Physics **88**, 4257 (2000).
[5]J. Dho, Y. N. Kim, Y. S. Hwang, J. C. Kim, and N. H. Hur, Applied Physics Letters **82**, 1434 (2003).
[6]J. D. Hoffman, B. J. Kirby, J. Kwon, G. Fabbris, D. Meyers, J. W. Freeland, I. Martin, O. G. Heinonen, P. Steadman, H. Zhou, C. M. Schlepütz, M. P. M. Dean, S. G. E. te Velthuis, J.-M. Zuo, and A. Bhattacharya, Physical Review X **6**, 041038 (2016).
[7]Z. Liao, M. Huijben, Z. Zhong, N. Gauquelin, S. Macke, R. J. Green, S. Van Aert, J. Verbeeck, G. Van Tendeloo, K. Held, G. A. Sawatzky, G. Koster, and G. Rijnders, Nature Materials **15**, 425 (2016).
[8]M. Ziese, I. Vrejoiu, E. Pippel, P. Esquinazi, D. Hesse, C. Etz, J. Henk, A. Ernst, I. V. Maznichenko, W. Hergert, and I. Mertig, Physical Review Letters **104**, 167203 (2010).
[9]D. Yi, J. Liu, S.-L. Hsu, L. Zhang, Y. Choi, J.-W. Kim, Z. Chen, J. D. Clarkson, C. R. Serrao, E. Arenholz, P. J. Ryan, H. Xu, R. J. Birgeneau, and R. Ramesh, Proceedings of the National Academy of Sciences **113**, 6397 (2016).
[10]J. Zhang, Z. Zhong, X. Guan, X. Shen, J. Zhang, F. Han, H. Zhang, H. Zhang, X. Yan, Q. Zhang, L. Gu, F. Hu, R. Yu, B. Shen, and J. Sun, Nature Communications **9**, 1923 (2018).
[11]Y.-M. Kim, J. He, M. D. Biegalski, H. Ambaye, V. Lauter, H. M. Christen, S. T. Pantelides, S. J. Pennycook, S. V. Kalinin, and A. Y. Borisevich, Nature Materials **11**, 888 (2012).
[12]J. T. Mefford, X. Rong, A. M. Abakumov, W. G. Hardin, S. Dai, A. M. Kolpak, K. P. Johnston, and K. J. Stevenson, Nature Communications **7**, 11053 (2016).
[13]M. A. Torija, M. Sharma, M. R. Fitzsimmons, M. Varela, and C. Leighton, Journal of Applied Physics **104**, 023901 (2008).
[14]T. L. Meyer, H. Jeen, X. Gao, J. R. Petrie, M. F. Chisholm, and H. N. Lee, Advanced Electronic Materials **2**, 1500201 (2015).
[15]J. Stöhr and H. C. Siegmann, in *Magnetism* 305–308 (Springer-Verlag, Berlin, Heidelberg, 2006).
[16]P. Bruno, Physical Review B **39**, 865 (1989).
[17]P. Bruno, *Magnetismus von Festkörpern und Grebzflächen 24.1–p* (KFA Jülich:Jülich, 1993).